JOURNAL OF GEOPHYSICAL RESEARCH: SOLID EARTH, VOL. 118, 4063–4070, doi:10.1002/jgrb.50324, 2013

Sulfur in olivine-hosted melt inclusions from the Emeishan picrites: Implications for S degassing and its impact on environment

Yan Zhang,[1,2] Zhong-Yuan Ren,[1] and Yi-Gang Xu [1]

Received 3 January 2013; revised 7 June 2013; accepted 2 August 2013; published 22 August 2013.

[1] Large-volume ($>0.3 \times 10^6$ km^3) basaltic lavas that erupted ~260 Ma ago in southwest China form the Emeishan large igneous province. The relationship between the Emeishan volcanism and the end-Guadalupian mass extinction is still unresolved. In order to evaluate the impact of Emeishan flood volcanism on the climate and environment, we have measured sulfur contents in olivine-hosted melt inclusions from Dali picrites. The highest S content of melt inclusions is up to 1311 ppm, which represents that of the undegassed magmas. Comparing the S contents in the undegassed magma and in the degassed posteruptive basaltic lavas, we calculate that eruptions of the Emeishan lavas could have released at least ~900 ppm of S, which equates to 5 Mt of SO_2 per cubic kilometer of basaltic lavas. During an individual eruption, SO_2 could have been added to the atmosphere at a rate of 1.5×10^2–10^3 Mt/yr, creating 3.1×10^2–10^3 Mt of H_2SO_4 aerosols. The quick release of such a huge amount of volatiles into the atmosphere may have absorbed and reflected solar radiation, causing a temperature decrease and eventually leading to a "volcanic winter". This scenario demonstrates that the Emeishan flood volcanism was responsible for the end-Guadalupian mass extinction.

Citation: Zhang, Y., Z.-Y. Ren, and Y.-G. Xu (2013), Sulfur in olivine-hosted melt inclusions from the Emeishan picrites: Implications for S degassing and its impact on environment, *J. Geophys. Res. Solid Earth*, *118*, 4063–4070, doi:10.1002/jgrb.50324.

1. Introduction

[2] Volcanic eruptions associated with large igneous provinces (LIPs) are, in many cases, considered coeval to crises in global climate and with mass extinctions [*Cockell*, 1999; *Olsen*, 1999; *Wignall*, 2001]. The apparent coincidence of the Siberian traps volcanism with the end-Permian mass extinction [*Bowring et al*., 1998; *Mundil et al*., 2004], the Deccan traps formation with the Cretaceous-Tertiary mass extinction [*Courtillot et al*., 1988; *Duncan and Pyle*, 1988], and the Columbia River basalt eruptions with a mid-Miocene extinction event [*Coffin and Eldholm*, 1994] suggest flood basalt eruptions may be responsible for some mass extinctions. The ~260 Ma Emeishan large igneous province (ELIP) in southwest China overlies and is interbedded with Middle-Late Permian carbonates that record the end-Guadalupian mass extinction. This implies a temporal coincidence between the end-Guadalupian mass extinction and the onset of Emeishan volcanism [*Courtillot et al*., 1999; *He et al*., 2007; *Zhou et al*., 2002], suggesting that there might be a cause-and-effect relationship between them [*He et al*., 2007; *Wignall*, 2001; *Wignall et al*., 2009; *Xu et al*., 2010]. However, the ''temporal coincidence'' is not yet certain whether the Emeishan volcanism was also leading to the end-Guadalupian mass extinction. The relationship between the Emeishan volcanism and the end-Guadalupian mass extinction yet remains to be resolved.

[3] Significant progress has been made recently as to the nature and origin of the Emeishan LIP, including a temporal-spatial distribution [e.g., *Fan et al*., 2008; *He et al*., 2007; *Zhong et al*., 2011], duration of magmatic activities [*Ali et al*., 2002; *He et al*., 2007; *Huang and Opdyke*, 1998; *Zheng et al*., 2010], geodynamic processes [e.g., *Chung and Jahn*, 1995; *He et al*., 2003; *Xu et al*., 2004, 2007], as well as carbon isotope [*Jin et al*., 2006; *Wang et al*., 2004; *Wignall et al*., 2009] and strontium isotope [*Jin et al*., 2006; *Wang et al*., 2004] excursions at the Lopingian-Guadalupian boundary. However to date, there have been almost no investigations on gases released during the Emeishan basalt eruption, which is critical to better understand the relationship between the Emeishan volcanism and the end-Guadalupian mass extinction.

[4] The onset of volcanism would have had a severe environmental impact, with the rapid release of huge amounts of gases (e.g., H_2O, CO_2, SO_2, Cl, and F) to the atmosphere capable of causing the mass extinction event [*Erwin*, 1994; *Officer et al*., 1987; *Pinto et al*., 1989; *Renne et al*., 1995; *Robock*, 2000; *Wignall*, 2001]. Of these volatiles, S gas, largely in the form of SO_2, has well-documented climatic, weather, and other environmental effects in modern basaltic eruptions [*Robock*, 2000; *Thordarson and Self*, 2003], as it reacts to produce atmospheric sulfate aerosol clouds. To explore whether S degassing during the formation of the ELIP is capable of being at least partly responsible for the end-Guadalupian mass extinction, we have measured S concentration in olivine-hosted melt inclusions, separated from

Additional supporting information may be found in the online version of this article.

[1]State Key Laboratory of Isotope Geochemistry, Guangzhou Institute of Geochemistry, Chinese Academy of Sciences, Guangzhou, China.
[2]University of Chinese Academy of Sciences, Beijing, China.

Corresponding author: Z.-Y. Ren, Guangzhou Institute of Geochemistry, Chinese Academy of Sciences, 511 Kehua St., Wushan, Guangzhou 510640, China. (zyren@gig.ac.cn)

2169-9313/13/10.1002/jgrb.50324

picrites collected from Dali, Yunnan province. Protected by their host crystals, melt inclusions are commonly not weathered and altered, therefore retaining information about preeruptive magma composition, especially mobile elements (e.g., volatile, alkali metal, and alkali-earth metal) [e.g., *Head et al*., 2011; *Kent*, 2008; *Thordarson and Self*, 1996].

[5] The data obtained in this study are compared with published S concentrations in melt inclusions from the Yongsheng and Binchuan picritic lavas in the ELIP. Based on S contents of melt inclusions and the residual S content of posteruptive basaltic lava, we estimate the minimum amount of S released during the Emeishan flood volcanism. These newly acquired data are used to evaluate the effect that volatiles released during the Emeishan flood volcanism would have on the environment, and whether the emplacement of the ELIP is responsible for the Permian mass extinctions.

2. Geological Background

[6] The Emeishan basalts are exposed across a rhombic-shaped area covering ~2.5×10^5 km^2 within Yunnan, Sichuan, and Guizhou Provinces, SW China (Figure S1) [*He et al*., 2003; *Huang and Opdyke*, 1998; *Xu et al*., 2001; *Zhang et al*., 2008]. With Mesozoic and Cenozoic complex tectonic events and block movements in SE Asia, the ELIP has been disrupted [*Chung et al*., 1997]. Late Permian volcanic rocks that can be correlated with those exposed in the ELIP have been reported in other regions, for example, in the Simao basin, Qiangtang terrane, the Jinping area, and the Song Da zone [*Chung et al*., 1998; *Song et al*., 2004; *Xiao et al*., 2003].

[7] The thickness of lavas varies from over 5 km in the west (e.g., in Yunnan Province) to several hundred meters in the east (e.g., in Guizhou Province) [*Xu et al*., 2001]. The entire volume of the Emeishan basalts is estimated to be ~0.3×10^6 km^3 [*Chung and Jahn*, 1995; *Hanski et al*., 2010; *Xu et al*., 2001]. However, this volume does not include the Emeishan-type basalts that have been traced in Qiangtang terrane and northern Vietnam. Therefore, this volume represents a minimum.

[8] Tholeiitic basalts make up more than 95% of the volume of the ELIP. *Xu et al*. [2001] and *Xiao et al*. [2004] classified the Emeishan basalts into two main types, high-Ti and low-Ti, based on Ti/Y ratios and TiO_2 contents. The low-Ti lavas are distributed at the base of the succession in the west, whereas the high-Ti lavas cover the whole area of the ELIP, dominating around the peripheries of the province [*Xiao et al*., 2004; *Xu et al*., 2001]. A recent study suggested that the ELIP lavas also have intermediate-Ti series with compositions between the low- and high-Ti end-members indicating that the magmatic series are continuous rather than discrete [*Kamenetsky et al*., 2012].

[9] The Emeishan massive volcanic successions lie uncomfortably over the early Late Permian Maokou formation and are overlain by the Late Permian Xuanwei/Longtan formation and Early Triassic or Jurassic strata [*He et al*., 2003, 2007; *Zhong et al*., 2007]. The Middle Permian platform limestones are succeeded by a volcanic pile with interbedded limestones, which record both a marine extinction and major C isotopic shift [*Wignall et al*., 2009]. Zircon ages from basalts and contemporaneous intrusions indicate that the volcanism occurred mainly at ~260 Ma [*Fan et al*., 2008; *Shellnutt and Zhou*, 2007; *Xu et al*., 2008; *Zhong et al*., 2011; *Zhou et al*., 2005, 2008]. These relative temporal relationships and absolute ages, together with the age of the Middle-Late Permian boundary (260.4 ± 0.4 Ma) [*Gradstein et al*., 2004], support a temporal link between the ELIP and the end-Guadalupian mass extinctions. Magnetostratigraphic studies suggest that the ELIP was emplaced over a short period of time (~1 Ma) [*Ali et al*., 2002; *Huang and Opdyke*, 1998; *Opdyke et al*., 2010], consistent with the lack of thick sedimentary piles or paleosols within the volcanic sections [*Xu et al*., 2001].

3. Samples and Methods

[10] Melt inclusions, tiny droplets of magma trapped in growing crystals, can provide a record of preeruptive volatile contents, such as S, Cl, F, H_2O, and CO_2 [*Devine et al*., 1984]. In this study, we analyzed the major element and volatile contents of 155 melt inclusions that occur in olivine grains from 12 picritic samples from Dali, Yunnan Province by electron microprobe. The melt inclusions compositions all belong to the intermediate-Ti type basalt [*Kamenetsky et al*., 2012]. We also considered published S concentration data for melt inclusions from the high-Ti (in the Yongsheng picrites) and low-Ti (in the Binchuan picrites) basalt types [*Kamenetsky et al*., 2012]. Detailed information, including sample locality and geochemistry of whole rock and melt inclusions has been presented elsewhere [*Hanski et al*., 2010; *Kamenetsky et al*., 2012]. The Dali picritic flows occur in a road cut ~20 km NE of the city of Dali (Figure S1), as reported by *Hanski et al*. [2010]. These samples are highly porphyritic (with 20–50 vol.% phenocrysts). They contain abundant phenocrysts of forsteritic olivine, plus minor clinopyroxene. The olivine phenocrysts are generally subhedral to euhedral, ranging from 0.4 to 2 mm across. Olivine is generally replaced by serpentine, but some grains retain cores of unaltered olivine (Figure S2a), many of which contain primary melt inclusions (Figure S2b). These melt inclusions mainly range from 10 to 100 μm in size and are spherical or oblate in shape. Sometimes, daughter mineral phases may appear in melt inclusions. These daughter minerals often have skeletal or dendritic textures indicating of rapid mineral growth (Figure S2b). Most inclusions also contain a vapor bubble (Figure S2c), which could have been trapped with the inclusion ("syngenetic" vapor bubble) or formed upon cooling ("shrinkage bubble") [*Hauri*, 2002]. Some olivine crystals also host Cr-spinel inclusions (Figure S2c).

[11] We handpicked olivine grains from crushed and sieved samples. To determine the chemical composition of trapped melts, it is almost always preferable to analyze a homogeneous glass rather than a mixture of various crystalline phases and residual glass. Prior to in situ microprobe analysis, the melt inclusions containing mixtures of crystals and glass require reheating and quenching in order to rehomogenize them as entirely glassy inclusions [*Danyushevsky et al*., 2000; *Hauri*, 2002; *Norman et al*., 2002; *Ren et al*., 2005; *Sobolev*, 1996]. We reheated olivine grains that contain melt inclusions using 1 atm furnaces. The condition of oxygen fugacity is maintained at the quartz-fayalite-magnetite (QFM) buffer with a CO_2:H_2 gas mixture. Samples were held at 1250°C for only 10 min in order to allow the daughter minerals to remelt, but not to allow volatiles to diffuse through the host olivine to the external melt [*Hauri*, 2002]. They were then rapidly quenched to homogeneous glassy inclusions. We mounted and polished

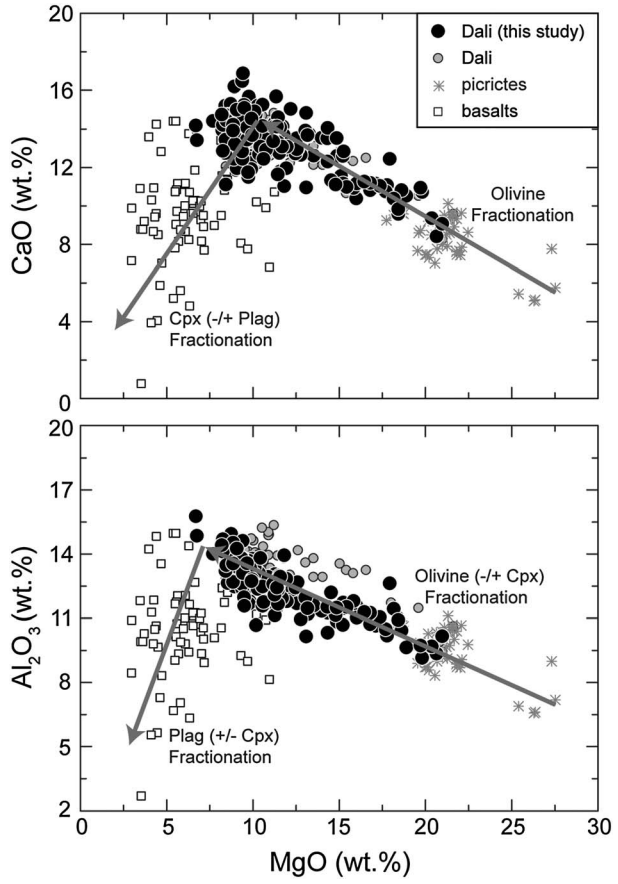

Figure 1. CaO and Al_2O_3 versus MgO contents (wt %) for the Dali melt inclusions (this study), other melt inclusions, and whole rock from the ELIP. Melts with MgO >10.5 wt % show variations consistent with only being controlled by olivine crystallization, whereas melt with MgO <10.5 wt % have began crystallize clinopyroxene, which will significantly change the FeO* content of the melt. Data for the Dali melt inclusions are from *Hanski et al*. [2010], and the whole rocks data are from *Hanski et al*. [2010], Ren, unpublished data, *Xiao et al*. [2004], and *Xu et al*., [2001].

individual reheated olivine grains until melt inclusions were exposed at the surface. All sample preparation was performed at the melt inclusion laboratory in the State Key Laboratory of Isotope Geochemistry, Guangzhou Institute of Geochemistry, Chinese Academy of Sciences (GIG-CAS). The preparation procedure of melt inclusions is described in detail by *Ren et al*. [2005].

[12] S concentrations and compositions of melt inclusions and their host olivines were analyzed using a JEOL JXA-8100 electron microanalysis at the State Key Laboratory of Isotope Geochemistry, GIG-CAS, following the method described by *Thordarson et al*. [1996]. The accelerating voltage was set at 15 kV with a beam current of 20 nA and 10 μm beam diameter for melt inclusions. The peak counting time was 400 s. The data reduction was carried out using the ZAF correction routine. The international glass standard NIST (National Institute of Standards and Technology) SRM 610 was analyzed as an unknown for S. The results show that the average S concentration of NIST SRM 610 is 508 ppm, and precision (SD) is 9 ppm, in good agreement with *Jochum et al*. [2011] and *Hauri et al*. [2002]. The analytical procedures of the compositions of the melt inclusions and olivine follow *Wang and Gaetani* [2008] and *Sobolev et al*. [2007], respectively. The relative analytical uncertainty (relative standard deviation) for the internal olivine standard is 0.1–0.4% for major elements (SiO_2, MgO, and FeO), 1–3% for minor elements (CaO, MnO, and NiO), and <0.5% (5, 1, and 8% for MnO, K_2O and P_2O_5, respectively) for most major elements in JB-2 (international basaltic standard). S and major element concentrations of the melt inclusions and the Fo contents of their host olivines are shown in Table S1.

4. Results

[13] The forsterite contents of olivines from the Dali picrites vary between 80.2 and 93.1 mol% (Table S1), encompassing the range of olivines from the Dali and Yongsheng picrites reported by *Kamenetsky et al*. [2012]. Melt inclusions display the so-called "Fe-loss" caused by postentrapment reequilibration with the host olivine. Once an inclusion has been trapped and the temperature decreases, crystallization of daughter mineral will commence [*Danyushevsky et al*., 2000; *Kent*, 2008; *Sobolev*, 1996]. The crystallization of the daughter mineral can be restored through reheating of the melt inclusion [*Danyushevsky et al*., 2000; *Hauri*, 2002; *Kent*, 2008]. However, "Fe-loss," which is the result of postentrapment diffusive reequilibration of Fe^{2+} and Mg between inclusion and host olivine, cannot be reversed experimentally but can be corrected [*Danyushevsky et al*., 2000; 2002]. The measured data have been corrected to account for the Fe-loss, using the widely applied method of *Danyushevsky et al*. [2000] and recalculated to be in equilibrium with the host olivine by applying the model of *Ford et al*. [1983] using the PETROLOG software [*Danyushevsky*, 2001]. This calculation requires an independent estimate of the initial trapped melt FeO* content, which in most cases can be estimated from the FeO* fractionation trend of the whole rocks [*Danyushevsky et al*., 2000, 2002]. According to the FeO* fractionation trend of the whole rocks, we set 10.8 wt % of total FeO for the initial trapped melt. The corrected S and other major elements compositions are listed in Table S1.

[14] After correction for olivine growth and Fe-Mg exchange between melt inclusion and its host olivine, when the melt inclusions with >10–11 wt % MgO are considered, both Al_2O_3 and CaO increase with decreasing MgO, which indicate that the magma fractionation trend is only controlled by olivine. Below 10 wt % MgO, as MgO decreases CaO decreases but Al_2O_3 still increases, suggesting fractionation of clinopyroxene without plagioclase fractionation; plagioclase begins to crystallize at lower MgO contents (Figure 1). Similar results have been reported by *Hanski et al*. [2010] and *Kamenetsky et al*. [2012]. *Hanski et al*. [2010] studied melt inclusions in the Dali picrites and interpreted that the compositions of melt inclusions are controlled by olivine and clinopyroxene fractionation, and clinopyroxene is crystallized at MgO contents <~12 wt %. Based on the compositions of melt inclusions from the Yongsheng, Binchuan, Lijiang, and Dali picrites, and the whole rocks, *Kamenetsky et al*. [2012] indicated that the knee points of fractionation trends for olivine and clinopyroxene are ~10 wt % MgO. When the melts evolve to MgO contents below 10–11 wt %, the crystallization of clinopyroxene and/or plagioclase will

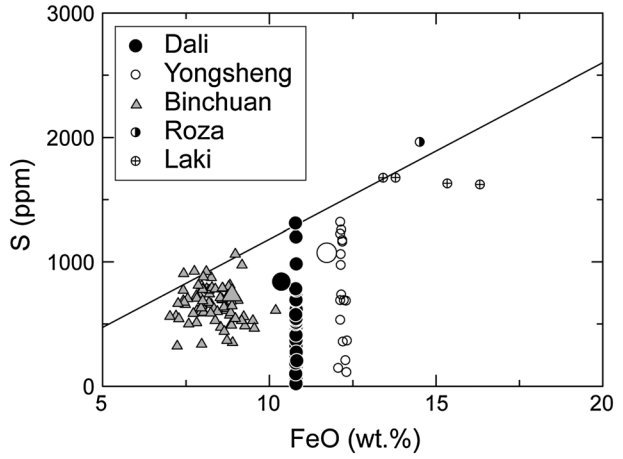

Figure 2. Plot of S versus FeO* (total Fe as FeO*) content for the melt inclusions. The solid line defines the submarine tholeiitic basalt FeS-saturation curve [S (wt. %) = 0.01418FeO* (wt %) - 0.02381] [*Blake et al*., 2010]. The high S contents of melt inclusions from Dali and Yongsheng picritic lavas plot near the submarine tholeiitic basalt FeS-saturation curve, indicating sulfur-saturation at the time of entrapment. All melt inclusions from the ELIP have MgO content >10.5 wt %, for detailed explanation see text. Large symbols represent S contents of the parental magmas of Binchuan, Dali, and Yongsheng. Data for Yongsheng melt inclusions are from *Kamenetsky et al*. [2012]. Data for Laki and Roza are from *Thordarson et al*. [1996] and *Thordarson and Self* [1996], respectively.

significantly change basaltic magma FeO* content. As a result, using the whole rock FeO* fractionation trend to set the FeO* content of the melt inclusions may be incorrect. Therefore, in this study, we only consider the data from melt inclusions with MgO >10.5 wt %, because these compositions are only controlled by olivine fractionation, and the FeO* content in melt inclusions will not change significantly. In those inclusion with MgO <10.5 wt %, FeO* content will be changed by clinopyroxene and/or plagioclase fractionation and will not equal the set value of FeO* content based on the whole rock FeO* fractionation trend.

[15] The remaining melt inclusions are much closer to primary compositions than other ELIP basaltic lavas [e.g., *Fan et al*., 2008; *Qi and Zhou*, 2008; *Xiao et al*., 2004; *Xu et al*., 2001] and lie on the evolutionary line defined by their host picritic lavas and those lavas (Figure 1). For the 12 samples for which we present data, S concentrations in melt inclusions range from below the detection limit (25 ppm) to 1311 ppm, with a range at any given MgO content (Table S1).

[16] High S inclusions could be trapped at an early stage of crystallization, whereas inclusions with low S contents could be trapped after significant degree of degassing [*Blake et al*., 2010; *Hauri*, 2002; *Kent*, 2008]. Some inclusions from the Dali picrites have high S concentrations (up to 1311 ppm; Table S1), which were trapped before degassing and could be representative of preeruptive magmas. In Figure 2, melt inclusions from the Dali and Binchuan picrites with high S contents plot near the submarine tholeiitic basalt FeS-saturation curve. Although some melt inclusions (MgO >10.5 wt %) from the Yongsheng picrites plot beneath the submarine tholeiitic basalt FeS-saturation curve, other melt inclusions (MgO <10.5 wt %) have higher S contents up to 1856 ppm [*Kamenetsky et al*., 2012], which might be sulfur saturated. Consequently, this indicates that these preeruption magmas are sulfur saturated at the time of entrapment. Most Emeishan melt inclusions have low S concentrations, suggesting that they were trapped in crystals that grew after the magma had already partially degassed, possibly in the conduit en route to the surface [*Blake et al*., 2010; *Hauri*, 2002; *Self et al*., 2008]. Some inclusions have even lower S concentrations (<400 ppm), which may be ascribed to volatile escape along microcracks that link these inclusions to the external melt [*Blake et al*., 2010; *Hauri*, 2002].

[17] Melt inclusions from the Binchuan picritic lavas, which belong to the low-Ti series, display slightly lower S contents (<1100 ppm) than those of Dali and Yongsheng, which are intermediate- and high-Ti series, respectively (Figure 2) [*Kamenetsky et al*., 2012]. Melt inclusions in the Binchuan picrites are hosted within chromian spinels [*Kamenetsky et al*., 2012]. Their lower S contents would be caused by lower FeO* [*Blake et al*., 2010; *Hauri*, 2002; *Wallace and Carmichael*, 1992] and can be ascribed to magma degassing before entrapment which is quite common in the high- and intermediate-Ti melt inclusions during magma evolution. Moreover, an undegassed composition might not have been sampled in the Binchuan inclusions due to the limited number found (nine data with MgO >10.5 wt %). Therefore, the lower S content of melt inclusions from the Binchuan picrites may not represent that of preeruptive low-Ti basalt. For the Dali and Yongsheng picrites, the highest S in inclusions with MgO >10.5 wt % is 1311 ppm (10.6 wt % of MgO) and 1320 ppm (13.9 wt % of MgO), respectively [*Kamenetsky et al*., 2012]. These could have been trapped before degassing and be representative of preeruptive magmas. Because increasing degrees of differentiation will cause the S concentrations in basaltic magmas to increase [*Wallace and Carmichael*, 1992], it is concluded that high-Ti basalts have higher S content than intermediate-Ti basalts before eruption at a given MgO. The high-Ti series are the dominant magma type covering the whole area of ELIP [*Xiao et al*., 2004; *Xu et al*., 2001]. Therefore, we can use the S content in the Dali melt inclusions to calculate and obtain the minimal amount of S released by the Emeishan basalt eruptions.

[18] We have estimated the parental magma compositions for each of the high-, intermediate- and low-Ti basalts. In each case, the melt inclusion with MgO >10.5 wt % containing the most S was used. The selected major elemental data of melt inclusions are adjusted to a constant Fe^{2+}/Fe^{3+} ratio of 0.9 (QFM buffer condition), and then olivine was added in 0.1% increments until the olivine composition in equilibrium with melt inclusions reached the most forsteritic olivine composition found in each basalt type [*Kamenetsky et al*., 2012]. The calculated parental magmas for the high-, intermediate-, and low-Ti basalts contain 19.50 wt %, 20.90 wt %, and 13.92 wt % MgO, with S contents of at least 1076 ppm, 844 ppm, and 762 ppm, respectively (Figure 2).

[19] S concentrations in melt inclusions from the Emeishan basalts are slightly less than those inferred during the eruption of the Laki lavas in Iceland, and the Roza lavas in the Columbia River province, United States (Figure 2). For instance, in the case of Laki (erupted from 1783–1784 AD),

S content in preeruptive magma are estimated to be ≤1700 ppm (average of 1677 ppm) [*Thordarson et al*., 1996]; Roza lavas, which erupted at ~15 Ma, are estimated to have preeruptive S contents of ≤1500 ppm (average of 1370 ppm) [*Thordarson and Self*, 1996]. The higher S concentrations in the Laki and Roza lavas may be ascribed to their relatively evolved nature (MgO <6 wt % compared to 7–21 wt % MgO in the Dali melt inclusions). If the lava is a fairly evolved basalt or basaltic andesite (<5 to 7 wt % MgO), and the magma was reduced (at or below the QFM buffer), then the magma is likely to be sulfide-saturated [*Blake et al*., 2010], and may have higher S concentrations comparable with sulfide-undersaturated magma. Alternatively, the Dali melt inclusions have lower total Fe contents (~10.9 wt %) than the Laki and Roza lavas, which may also result in the Dali melt inclusions having lower dissolved S concentrations (Figure 2). Therefore, in the case of the ELIP, where lavas are dominated by rocks with MgO <7 wt % and FeO* >12 wt %, magmas would dissolve far more than 1311 ppm of S before degassing.

5. Discussion

5.1. Degassing From the Emeishan Basalts

[20] S emissions from past eruptions can be estimated by comparing S concentrations in melt inclusions, which may represent S concentrations in preeruptive magma, with S concentrations that remain in the glassy tephra or lava after degassing. This is called the "petrologic method" [*Devine et al*., 1984]. However, the application of the "petrologic method" is limited for crystal-poor and/or weathered/altered lavas, because weathering or low-temperature alteration can change the contents of mobile volatile elements in rocks [*Self et al*., 2005]. The Emeishan lavas, formed at ~260 Ma, have typically been affected by weathering and low-temperature alteration. Therefore, we cannot directly obtain the posteruptive S concentrations in the matrix glasses of the Emeishan lavas. Many analyses of S contents have been done on fresh tholeiitic basaltic glasses in scoria and quenched lavas. *Blake et al*. [2010] collected and summarized S concentrations of historic and other youthful scoria and lavas and gave an average value of 400 ± 200 ppm in basaltic lavas. Here we use this average value as the posteruptive S concentration remaining in the Emeishan lavas.

[21] For the purposes of this paper, we express the Emeishan SO_2 emission as the mass of gas released at the vents per cubic kilometer of magma erupted. From mass balance, this can be estimated by

$$M_{\mathrm{rel}} = 2M_{\mathrm{m}}\left(C_{\mathrm{inc}} - C_{\mathrm{gl}}\right) \quad (1)$$

where M_{rel} is the mass of SO_2 released at the vent in kg, M_{m} is the mass of magma in kg, C_{inc} and C_{gl} are the concentrations of S in melt inclusions (representing the preeruptive S content) and in vent tephra (representing the posteruptive S content), respectively, and the factor of 2 accounts for the difference between the atomic masses of S and SO_2. Using the difference between the highest S concentration in an inclusion (1311 ppm, the S content of preeruptive magma) and the average S concentration in lavas (400 ppm, the remained S content of posteruptive magma), the amount of S degassed amounts to ~900 ppm. Thus, assuming a magma density of 2750 kg m^{-3} [*Metrich et al*., 1991] for every 1 km^3 of erupted magma, an average of 5 Mt (1 Mt = 10^{12} g) of SO_2 was released at the vents.

[22] Using the equation proposed by *Blake et al*. [2010, equation 3], and whole rock FeO* of Dali picrites of ~10.8 wt % (Zhong-Yuan Ren et al., unpublished data), we have calculated the S yield from the Emeishan basalt eruptions. The result shows that the S yield is 890 ppm, and thus every 1 km^3 of Emeishan basalts can release 4.913 Mt of SO_2 into atmosphere. The amounts of S released by Emeishan basalts, calculated using these two different methods, are consistent with each other within error. The SO_2 released per cubic kilometer of Emeishan lava is a bit lower than that calculated for the Roza lavas (SO_2, 7 Mt/km^3) [*Thordarson and Self*, 1996]. As mentioned above, this may be due to the melts which are used to estimate the preeruptive S concentration being relatively primitive and thus having lower FeO* contents.

[23] The volume of Emeishan basalts was estimated to be $>0.3 \times 10^6$ km^3 [*Chung and Jahn*, 1995; *Hanski et al*., 2010; *Xu et al*., 2001]. Therefore, at least 1.5×10^6 Mt of SO_2 was released into the atmosphere during the formation of the ELIP. The released SO_2 from the ELIP is roughly 1/10 of that estimated to have been released by the Siberian Traps ($1.26–1.56 \times 10^7$ Mt SO_2 from 4×10^6 km^3 basaltic lavas [*Black et al*., 2012]) and slightly higher than that from the Columbia River province (1.0×10^6 Mt SO_2 from 0.15×10^6 km^3 lavas [*Blake et al*., 2010]).

5.2. Environmental Impact

[24] The presence of pyoclastic rock and vesiculate basalts in the ELIP [*Lin*, 1985; *Ross et al*., 2005; *Wignall et al*., 2009] suggests that the forceful, violent phreatomagmatic-style volcanism is typical of much of the early to midstages of the Emeishan volcanism [*Wignall et al*., 2009]. This is evidence that the Emeishan basalts eruptions not only pour out a huge amount of lava but also release a large amount of gas.

[25] Flood basalt volcanism can influence the environment either by climatic cooling effects caused by increasing atmospheric optical density as a result of SO_2 release and sulphuric acid aerosol formation or by atmospheric warming through the addition of the greenhouse gases, e.g., CO_2 [*McLean*, 1985; *Olsen*, 1999]. In order to estimate the effects of the gas released by the ELIP, we need to know the amount of SO_2 and CO_2 released on eruption (including magmatic CO_2 and sediment-derived CO_2).

[26] CO_2 is relatively insoluble in basaltic melts [*Saal et al*., 2002], and CO_2 content in basaltic lavas is not more than 0.5 wt % [*Wallace and Anderson*, 2000]. If the preeruption CO_2 content of the Emeishan basalts was 0.5 wt %, and it completely degassed from the magma during eruption, 4.13×10^6 Mt of magmatic CO_2 would have been released into the atmosphere. In addition, the mass of sediment-derived CO_2 formed by reaction between mafic intrusions, that were coeval with the eruption of the Emeishan basalts, and the limestone wall rocks is ~3.6 to 8.6 times larger than the mass of magmatic CO_2 [*Ganino and Arndt*, 2009]. Therefore, during the Emeishan basalt eruptions, 1.49×10^7 to 3.55×10^7 Mt of sediment-derived CO_2 would have been formed, giving a total CO_2 emission of 1.9×10^7 to 4.0×10^7 Mt.

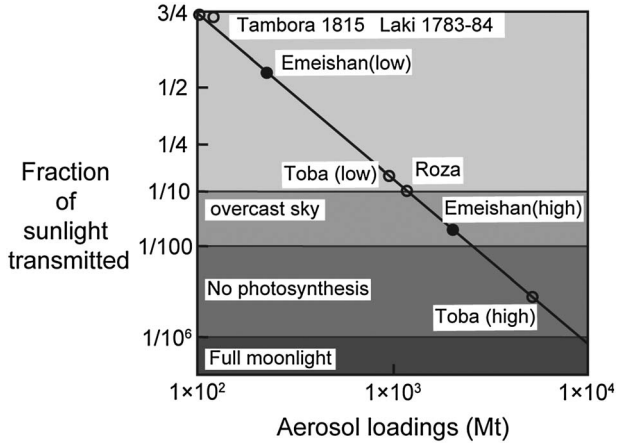

Figure 3. Fraction of sunlight transmitted through aerosols and/or fine-ash clouds of different masses. Modified from *Thordarson and Self* [1996]. The lowest sulfate loading calculated for the ELIP is larger than that of Laki. The highest loading would restrict the amount of transmitted sunlight to levels similar to that experienced with an overcast sky; levels of sunlight low enough to lead to a severe "volcanic winter."

[27] Large igneous provinces formed by main pulses of eruptive activity [*Rampino and Stothers*, 1988] over a short period of geologic time (~1 Ma) consist of many large volume and prolonged eruptions, each huge eruption commonly yielding lava flow fields of 10^2–10^3 km^3, lasting about a decade or more, and spaced hundreds to thousands of years apart [*Bryan et al*., 2010; *Self et al*., 2005]. If this situation is also applicable to the ELIP, and each eruption yields lava fields of 3×10^2–10^3 km^3, the total CO_2 released would have been about 1.9×10^4 to 4.0×10^5 Mt, and the average annual ejection of CO_2 into the atmosphere would have been about 1.9×10^3 to 4.0×10^4 Mt. This value, however, close to, or below the current anthropogenic CO_2 release of 10^4 Mt/yr [*Leavitt*, 1982; *Sigurdsson*, 1990], and both values are tiny compared to the 5×10^7 Mt C in the atmosphere and oceans [*Wignall*, 2001]. It is therefore unlikely that magmatic and sediment-derived CO_2 released by the ELIP eruptions would have resulted in notable global warming.

[28] During decade-long Emeishan basalt eruption, 1.5×10^3–10^4 Mt of SO_2 would have been released. This could have resulted in a sustained atmospheric loading of 1.5×10^2–10^3 Mt/yr over the duration of the eruption, assuming constant effusion rates. Such fluxes of S gas are enormous when compared with anthropogenic SO_2 released into atmosphere (10 Mt/yr) and the background amount of S in the atmosphere (<1 Mt) [*Self et al*., 2006], and the impact upon the atmosphere and climate are likely to have been significant. Theoretically, SO_2 will react with water vapor to form sulfate aerosols. If SO_2 converts into H_2SO_4 completely, it yields 3.1×10^6 Mt of sulfuric aerosols, assuming a composition of 75 wt % H_2SO_4 and 25 wt % H_2O for the aerosols [*Thordarson and Self*, 2003]. These aerosols will form a veil in the tropopause or lower stratosphere, blocking solar radiation from reaching the surface and resulting in abnormal climate phenomena.

[29] Flood basalt eruption column heights could exceed 13 km, reaching middle to upper-troposhperic altitudes at tropical to midlatitudes, or even the base of the stratosphere at higher latitudes or during higher intensity eruptions [*Self et al*., 2005; 2006]. The residence time of an average aerosol particle (radius = 0.3 μm) in the upper troposphere and the lower stratosphere is on the order of 50 to 400 days [*Jaenicke*, 1984]. According to the previous calculation, an individual Emeishan basalt eruption could have released 3.1×10^2–10^3 Mt/yr of sulfuric aerosols into the atmosphere for a decade or more. Although such huge amounts of aerosols will fall out of the atmosphere fast, they could be resupplied by continuous SO_2 emissions [*Thordarson and Self*, 1996]. Therefore, we estimate that the ELIP maintained an annual atmospheric H_2SO_4 loading in the range of 100–1500 Mt. If the aerosol cloud is dispersed around the globe, then the optical thickness of the cloud can be estimated from

$$\tau_D = \frac{9QM_D}{32\pi R^2 r\rho} \tag{2}$$

where τ_D is optical depth, M_D is the aerosol mass, R is the radius of the Earth, Q is an efficiency factor for scattering and absorption by the aerosol particles, and r and ρ are the aerosol particle radius and density, respectively [*Stothers*, 1984; *Thordarson and Self*, 1996]. Using typical modal values of $Q = 2$, $r = 3 \times 10^{-7}$ m, and $\rho = 1500$ kg m^{-3}, then the range of aerosol optical depths caused by the Emeishan aerosol clouds may have been 1–14. The opacity of the Emeishan aerosol clouds may have been similar to that of an overcast sky (Figure 3), and this could have lasted a decade or more. Such a scenario is similar to that predicted for a severe "volcanic winter."

[30] In addition to converting to aerosols, SO_2 will further form acid rain which may have been widespread. Moreover, a large amount of HCl and HF will also have been released into the atmosphere during the eruption. HF gas will adsorb onto the surface of ash particles, destroying and polluting vegetation and water, resulting in animal asphyxia and death [*Cockell*, 1999]. The potential damage caused by Cl includes the localized effects of acid rain and ozone depletion [*Cockell*, 1999].

[31] Therefore, the vast amount of S gas released during the Emeishan basalt eruptions could have had a severe impact on the climate and environment, and eventually led to the end-Guadalupian mass extinction.

6. Conclusions

[32] Although the Emeishan picritic lavas have undergone severe alteration, we still find a large number of residual olivine-hosted melt inclusions with S concentrations up to 1311 ppm. The mass balance calculation indicates that 1 km^3 of Emeishan basalts can release 5 Mt of SO_2 into the atmosphere. Thus, during the duration of the Emeishan basalt eruptions, a total of more than 1.5×10^6 Mt of SO_2 was released into the atmosphere. During a single Emeishan basalt eruption, 1.5×10^3–10^4 Mt of SO_2 would have been released into the atmosphere at an average rate of 1.5×10^2–10^3 Mt/yr for a decade. Assuming all the released SO_2 completely converted to aerosols, this would equate to the generation of 3.1×10^2–10^3 Mt of H_2SO_4 aerosols each year for a decade. This amount of aerosol loading into the atmosphere could cause 1–14 of aerosol optical depths, similar to that of an overcast sky, and enough to lead to a severe "volcanic

winter." Thus, the S gas emitted during the formation of the Emeishan LIP could have brought about abnormal climate phenomena across the middle-late Permian boundary, and eventually led to the end-Guadalupian mass extinction.

[33] **Acknowledgments.** We are grateful to Zhen-Yu Luo and Jiang-Bo Lan for their field assistance and Lei Wu for her help on melt inclusions preparation and microprobe analyses. We thank A.R.L. Nichols for valuable comments and help in improving the English. The paper benefited from helpful comments by the Editor M. Walter, Associate Editor C.-T. Lee, and P. J. Michael and an anonymous reviewer. The authors gratefully acknowledge the financial support from the National Basic Research Program of China (2011CB808903, 2011CB808906), the National Science Foundation of China (40873019), the "hundred talent project" of Chinese Academy of Sciences, and the Chinese Academy of Sciences Knowledge Innovation Program (KZCX2-YW-Q08-4). This is contribution No. IS-1727 from GIG-CAS.

References

Ali, J. R., G. M. Thompson, X. Y. Song, and Y. L. Wang (2002), Emeishan Basalts (SW China) and the 'end-Guadalupian' crisis: Magnetobiostratigraphic constraints, *J. Geol. Soc.*, *159*(1), 21–29, doi:10.1144/0016-764901086.

Black, B. A., L. T. Elkins-Tanton, M. C. Rowe, and I. U. Peate (2012), Magnitude and consequences of volatile release from the Siberian Traps, Earth Planet, *Sci. Lett.*, *317*, 363–373, doi:10.1016/j.epsl.2011.12.001.

Blake, S., S. Self, K. Sharma, and S. Sephton (2010), Sulfur release from the Columbia River Basalts and other flood lava eruptions constrained by a model of sulfide saturation, *Earth Planet. Sci. Lett.*, *299*(3–4), 328–338, doi:10.1016/j.epsl.2010.09.013.

Bowring, S. A., D. H. Erwin, Y. G. Jin, M. W. Martin, K. Davidek, and W. Wang (1998), U/Pb zircon geochronology and tempo of the end-Permian mass extinction, *Science*, *280*(5366), 1039–1045, doi:10.1126/science.280.5366.1039.

Bryan, S. E., I. U. Peate, D. W. Peate, S. Self, D. A. Jerram, M. R. Mawby, J. S. Marsh, and J. A. Miller (2010), The largest volcanic eruptions on Earth, *Earth Sci. Rev.*, *102*(3–4), 207–229, doi:10.1016/j.earscirev.2010.07.001.

Chung, S. L., and B. M. Jahn (1995), Plume-lithosphere interaction in generation of the Emeishan flood basalts at the Permian-Triassic boundary, *Geology*, *23*(10), 889–892, doi:10.1130/0091-7613(1995)023<0889:PLIIGO>2.3.CO;2.

Chung, S. L., T. Y. Lee, C. H. Lo, P. L. Wang, C. Y. Chen, N. T. Yem, T. T. Hoa, and G. Y. Wu (1997), Intraplate extension prior to continental extrusion along the Ailao Shan-Red River shear zone, *Geology*, *25*(4), 311–314, doi:10.1130/0091-7613(1997)025<0311:IEPTCE>2.3.CO;2.

Chung, S. L., B. M. Jahn, W. Genyao, C. H. Lo, and C. Bolin (1998), The Emeishan flood Basalt in SW China: A mantle plume initiation model and its connection with continental breakup and mass extinction at the Permian-Triassic boundary, in *Mantle Dynamics and Plate Interactions in East Asia, Geodyn. Ser*, edited by M. F. J. Flower, S. L. Chung, C. H. Lo, and T. Y. Lee, AGU, Washington, D. C., vol. 27, pp. 47–58.

Cockell, C. S. (1999), Crises and extinction in the fossil record - a role for ultraviolet radiation?, *Paleobiology*, *25*(2), 212–225.

Coffin, M. F., and O. Eldholm (1994), Large igneous provinces - Crustal structure, dimensions, and external consequences, *Rev. Geophys.*, *32*(1), 1–36, doi:10.1029/93rg02508.

Courtillot, V., G. Feraud, H. Maluski, D. Vandamme, M. G. Moreau, and J. Besse (1988), Deccan flood basalts and the cretaceous tertiary boundary, *Nature*, *333*(6176), 843–846, doi:10.1038/333843a0.

Courtillot, V., C. Jaupart, I. Manighetti, P. Tapponnier, and J. Besse (1999), On causal links between flood basalts and continental breakup, *Earth Planet. Sci. Lett.*, *166*(3–4), 177–195, doi:10.1016/S0012-821x(98)00282-9.

Danyushevsky, L. V. (2001), The effect of small amounts of H_2O on crystallisation of mid-ocean ridge and backarc basin magmas, *J. Volcanol. Geotherm. Res.*, *110*, 265–280.

Danyushevsky, L. V., F. N. Della-Pasqua, and S. Sokolov (2000), Re-equilibration of melt inclusions trapped by magnesian olivine phenocrysts from subduction-related magmas: Petrological implications, *Contrib. Mineral. Petrol.*, *138*(1), 68–83, doi:10.1007/pl00007664.

Danyushevsky, L. V., S. Sokolov, and T. J. Falloon (2002), Melt inclusions in olivine phenocrysts: Using diffusive re-equilibration to determine the cooling history of a crystal, with implications for the origin of olivine-phyric volcanic rocks, *J. Petrol.*, *43*(9), 1651–1671, doi:10.1093/petrology/43.9.1651.

Devine, J. D., H. Sigurdsson, A. N. Davis, and S. Self (1984), Estimates of sulfur and chlorine yield to the atmosphere from volanic eruptions and potential climatic effects, *J. Geophys. Res.*, *89*(B7), 6309–6325, doi:10.1029/JB089iB07p06309.

Duncan, R. A., and D. G. Pyle (1988), Rapid eruption of the Deccan flood basalts at the cretaceous tertiary boundary, *Nature*, *333*(6176), 841–843, doi:10.1038/333841a0.

Erwin, D. H. (1994), The Permo-Triassic extinction, *Nature*, *367*(6460), 231–236.

Fan, W. M., C. H. Zhang, Y. J. Wang, F. Guo, and T. P. Peng (2008), Geochronology and geochemistry of Permian basalts in western Guangxi Province, Southwest China: Evidence for plume-lithosphere interaction, *Lithos*, *102*(1–2), 218–236, doi:10.1016/j.lithos.2007.09.019.

Ford, C. E., D. G. Russell, J. A. Craven, and M. R. Fisk (1983), Olivine liquid equilibria – Temperature, pressure and composition dependence of the crystal liquid cation partition-coefficients for Mg, Fe^{2+}, Ca and Mn, *J. Petrol.*, *24*(3), 256–265.

Ganino, C., and N. T. Arndt (2009), Climate changes caused by degassing of sediments during the emplacement of large igneous provinces, *Geology*, *37*(4), 323–326, doi:10.1130/G25325A.1.

Gradstein, F. M., J. G. Ogg, A. G. Smith, W. Bleeker, and L. J. Lourens (2004), A new geologic time scale, with special reference to Precambrian and Neogene, *Episodes*, *27*(2), 83–100.

Hanski, E., V. S. Kamenetsky, Z. Y. Luo, Y. G. Xu, and D. V. Kuzmin (2010), Primitive magmas in the Emeishan large igneous province, southwestern China and northern Vietnam, *Lithos*, *119*(1–2), 75–90, doi:10.1016/j.lithos.2010.04.008.

Hauri, E. (2002), SIMS analysis of volatiles in silicate glasses, 2: Isotopes and abundances in Hawaiian melt inclusions, *Chem. Geol.*, *183*(1–4), 115–141, doi:10.1016/S0009-2541(01)00374-6.

Hauri, E., J. H. Wang, J. E. Dixon, P. L. King, C. Mandeville, and S. Newman (2002), SIMS analysis of volatiles in silicate glasses 1. Calibration, matrix effects and comparisons with FTIR, *Chem. Geol.*, *183*(1–4), 99–114, doi:10.1016/S0009-2541(01)00375-8.

He, B., Y. G. Xu, S. L. Chung, L. Xiao, and Y. M. Wang (2003), Sedimentary evidence for a rapid, kilometer-scale crustal doming prior to the eruption of the Emeishan flood basalts, *Earth Planet. Sci. Lett.*, *213*(3–4), 391–405, doi:10.1016/S0012-821X(03)00323-6.

He, B., Y. G. Xu, X. L. Huang, Z. Y. Luo, Y. R. Shi, Q. J. Yang, and S. Y. Yu (2007), Age and duration of the Emeishan flood volcanism, SW China: Geochemistry and SHRIMP zircon U–Pb dating of silicic ignimbrites, post-volcanic Xuanwei formation and clay tuff at the Chaotian section, *Earth Planet. Sci. Lett.*, *255*(3–4), 306–323, doi:10.1016/j.epsl.2006.12.021.

Head, E. M., A. M. Shaw, P. J. Wallace, K. W. W. Sims, and S. A. Carn (2011), Insight into volatile behavior at Nyamuragira volcano (D.R. Congo, Africa) through olivine-hosted melt inclusions, *Geochem. Geophys. Geosyst.*, *12*, Q0AB11, doi:10.1029/2011gc003699.

Huang, K. N., and N. D. Opdyke (1998), Magnetostratigraphic investigations on an Emeishan basalt section in western Guizhou province, China, *Earth Planet. Sci. Lett.*, *163*(1–4), 1–14, doi:10.1016/S0012-821X(98)00169-1.

Jaenicke, R. (1984), Physical aspects of the atmospheric aerosol, in *Aerosols and Their Climatic Effects*, edited by H. E. Gerber and A. Deepak, A. Deepak, Hampton, pp. 7–34.

Jin, Y. G., S. Z. Shen, C. M. Henderson, X. D. Wang, W. Wang, Y. Wang, C. Q. Cao, and Q. H. Shang (2006), The Global Stratotype Section and Point (GSSP) for the boundary between the Capitanian and Wuchiapingian stage (Permian), *Episodes*, *29*(4), 253–262.

Jochum, K. P., et al. (2011), Determination of reference values for NIST SRM 610–617 glasses following ISO guidelines, *Geostand. Geoanal. Res.*, *35*(4), 397–429, doi:10.1111/j.1751-908X.2011.00120.x.

Kamenetsky, V. S., S. L. Chung, M. B. Kamenetsky, and D. V. Kuzmin (2012), Picrites from the Emeishan large igneous province, SW China: A compositional continuum in primitive magmas and their respective mantle sources, *J. Petrol.*, *53*(10), 2095–2113, doi:10.1093/petrology/egs045.

Kent, A. J. R. (2008), Melt inclusions in basaltic and related volcanic rocks, *Rev. Mineral. Geochem.*, *69*(1), 273–331, doi:10.2138/rmg.2008.69.8.

Leavitt, S. (1982), Annual volcanic carbon dioxide emission: An estimate from eruption chronologies, *Environ. Geol.*, *4*(1), 15–21, doi:10.1007/BF02380495.

Lin, J. Y. (1985), Spatial and temporal distribution of Emeishan basaltic rocks in three southwestern province (Sichuan, Yunnan and Guizhou) of China, *Chin. Sci. Bull.*, *12*, 929–932.

McLean, D. M. (1985), Deccan traps mantle degassing in the terminal Cretaceous marine extinctions, *Cretac. Res.*, *6*(3), 235–259, doi:10.1016/0195-6671(85)90048-5.

Metrich, N., H. Sigurdsson, P. S. Meyer, and J. D. Devine (1991), The 1783 Lakagigar eruption in Iceland: Geochemistry, CO_2 and sulfur degassing, *Contrib. Mineral. Petrol.*, *107*(4), 435–447, doi:10.1007/bf00310678.

Mundil, R., K. R. Ludwig, I. Metcalfe, and P. R. Renne (2004), Age and timing of the Permian mass extinctions: U/Pb dating of closed-system zircons, *Science*, *305*(5691), 1760–1763, doi:10.1126/science.1101012.

Norman, M. D., M. O. Garcia, V. S. Kamenetsky, and R. L. Nielsen (2002), Olivine-hosted melt inclusions in Hawaiian picrites: Equilibration, melting, and plume source characteristics, *Chem. Geol.*, *183*(1–4), 143–168, doi:10.1016/S0009-2541(01)00376-X.

Officer, C. B., A. Hallam, C. L. Drake, and J. D. Devine (1987), Late Cretaceous and paroxysmal Cretaceous/Tertiary extinctions, *Nature*, *326*(6109), 143–149.

Olsen, P. E. (1999), Giant lava flows, mass extinctions, and mantle plumes, *Science*, *284*(5414), 604–605, doi:10.1126/science.284.5414.604.

Opdyke, N. D., D. V. Kent, K. N. Huang, D. A. Foster, and J. P. Patel (2010), Equatorial paleomagnetic time-averaged field results from 0–5 Ma lavas from Kenya and the latitudinal variation of angular dispersion, *Geochem. Geophys. Geosyst.*, *11*, Q05005, doi:10.1029/2009GC002863.

Pinto, J. P., R. P. Turco, and O. B. Toon (1989), Self-limiting physical and chemical effects in volcanic eruption clouds, *J. Geophys. Res.*, *94*(D8), 11,165–11,174, doi:10.1029/JD094iD08p11165.

Qi, L., and M. F. Zhou (2008), Platinum-group elemental and Sr-Nd-Os isotopic geochemistry of Permian Emeishan flood basalts in Guizhou Province, SW China, *Chem. Geol.*, *248*(1–2), 83–103, doi:10.1016/j.chemgeo.2007.11.004.

Rampino, M. R., and R. B. Stothers (1988), Flood basalt volcanism during the past 250 million years, *Science*, *241*(4866), 663–668, doi:10.1126/science.241.4866.663.

Ren, Z. Y., S. Ingle, E. Takahashi, N. Hirano, and T. Hirata (2005), The chemical structure of the Hawaiian mantle plume, *Nature*, *436*(7052), 837–840, doi:10.1038/nature03907.

Renne, P. R., M. T. Black, Z. C. Zhang, M. A. Richards, and A. R. Basu (1995), Synchrony and causal relations between Permian-Triassic boundary crises and Siberian flood volcanism, *Science*, *269*(5229), 1413–1416, doi:10.1126/science.269.5229.1413.

Robock, A. (2000), Volcanic eruptions and climate, *Rev. Geophys.*, *38*(2), 191–219, doi:10.1029/1998rg000054.

Ross, P. S., I. U. Peate, M. K. McClintock, Y. G. Xu, I. P. Skilling, J. D. L. White, and B. F. Houghton (2005), Mafic volcaniclastic deposits in flood basalt provinces: A review, *J. Volcanol. Geotherm. Res.*, *145*(3–4), 281–314, doi:10.1016/j.jvolgeores.2005.02.003.

Saal, A. E., E. H. Hauri, C. H. Langmuir, and M. R. Perfit (2002), Vapour undersaturation in primitive mid-ocean-ridge basalt and the volatile content of Earth's upper mantle, *Nature*, *419*(6906), 451–455, doi:10.1038/nature01073.

Self, S., T. Thordarson, and M. Widdowson (2005), Gas fluxes from flood basalt eruptions, *Elements*, *1*(5), 283–287, doi:10.2113/gselements.1.5.283.

Self, S., M. Widdowson, T. Thordarson, and A. E. Jay (2006), Volatile fluxes during flood basalt eruptions and potential effects on the global environment: A Deccan perspective, *Earth Planet. Sci. Lett.*, *248*(1–2), 518–532, doi:10.1016/j.epsl.2006.05.041.

Self, S., S. Blake, K. Sharma, M. Widdowson, and S. Sephton (2008), Sulfur and chlorine in late Cretaceous Deccan magmas and eruptive gas release, *Science*, *319*(5870), 1654–1657, doi:10.1126/science.1152830.

Shellnutt, J. G., and M. F. Zhou (2007), Permian peralkaline, peraluminous and metaluminous A-type granites in the Panxi district, SW China: Their relationship to the Emeishan mantle plume, *Chem. Geol.*, *243*(3–4), 286–316, doi:10.1016/j.chemgeo.2007.05.022.

Sigurdsson, H. (1990), Evidence of volcanic loading of the atmosphere and climate response, *Paleogeogr. Paleoclimatol. Paleoecol.*, *89*(3), 277–289.

Sobolev, A. V. (1996), Melt inclusions in minerals as a source of principle petrological information, *Petrology*, *4*(3), 209–220.

Sobolev, A. V., et al. (2007), The amount of recycled crust in sources of mantle-derived melts, *Science*, *316*(5823), 412–417, doi:10.1126/science.1138113.

Song, X. Y., M. F. Zhou, Z. M. Cao, and P. T. Robinson (2004), Late Permian rifting of the South China Craton caused by the Emeishan mantle plume?, *J. Geol. Soc.*, *161*, 773–781, doi:10.1144/0016-764903-135.

Stothers, R. B. (1984), The great Tambora eruption in 1815 and its aftermath, *Science*, *224*(4654), 1191–1198, doi:10.1126/science.224.4654.1191.

Thordarson, T., and S. Self (1996), Sulfur, chlorine and fluorine degassing and atmospheric loading by the Roza eruption, Columbia River Basalt Group, Washington, USA, *J. Volcanol. Geotherm. Res.*, *74*(1–2), 49–73, doi:10.1016/s0377-0273(96)00054-6.

Thordarson, T., and S. Self (2003), Atmospheric and environmental effects of the 1783–1784 Laki eruption: A review and reassessment, *J. Geophys. Res.*, *108*(D1), 4011, doi:10.1029/2001jd002042.

Thordarson, T., S. Self, N. Óskarsson, and T. Hulsebosch (1996), Sulfur, chlorine, and fluorine degassing and atmospheric loading by the 1783–1784 AD Laki (Skaftár Fires) eruption in Iceland, *Bull. Volcanol.*, *58*(2), 205–225, doi:10.1007/s004450050136.

Wallace, P. J., and A. F. Anderson (2000), Volatiles in magmas, in *Encyclopedia of Volcanoes*, edited by H. Sigurdsson, Wiley, New York, pp. 149–163.

Wallace, P., and I. S. E. Carmichael (1992), Sulfur in basaltic magmas, *Geochim. Cosmochim. Acta*, *56*(5), 1863–1874.

Wang, W., C. Q. Cao, and Y. Wang (2004), The carbon isotope excursion on GSSP candidate section of Lopingian-Guadalupian boundary, *Earth Planet. Sci. Lett.*, *220*(1–2), 57–67, doi:10.1016/S0012-821x(04)00033-0.

Wang, Z. R., and G. A. Gaetani (2008), Partitioning of Ni between olivine and siliceous eclogite partial melt: Experimental constraints on the mantle source of Hawaiian basalts, *Contrib. Mineral. Petrol.*, *156*(5), 661–678, doi:10.1007/s00410-008-0308-y.

Wignall, P. B. (2001), Large igneous provinces and mass extinctions, *Earth Sci. Rev.*, *53*(1–2), 1–33, doi:10.1016/S0012-8252(00)00037-4.

Wignall, P. B., et al. (2009), Volcanism, mass extinction, and carbon isotope fluctuations in the middle Permian of China, *Science*, *324*(5931), 1179–1182, doi:10.1126/science.1171956.

Xiao, L., Y. G. Xu, S. L. Chung, B. He, and H. J. Mei (2003), Chemostratigraphic correlation of Upper Permian Lavas from Yunnan Province, China: Extent of the Emeishan large igneous province, *Int. Geol. Rev.*, *45*(8), 753–766, doi:10.2747/0020-6814.45.8.753.

Xiao, L., Y. G. Xu, H. J. Mei, Y. F. Zheng, B. He, and F. Pirajno (2004), Distinct mantle sources of low-Ti and high-Ti basalts from the western Emeishan large igneous province, SW China: Implications for plume–lithosphere interaction, *Earth Planet. Sci. Lett.*, *228*(3–4), 525–546, doi:10.1016/j.epsl.2004.10.002.

Xu, Y. G., S. L. Chung, B. M. Jahn, and G. Y. Wu (2001), Petrologic and geochemical constraints on the petrogenesis of Permian–Triassic Emeishan flood basalts in southwestern China, *Lithos*, *58*(3–4), 145–168, doi:10.1016/S0024-4937(01)00055-X.

Xu, Y. G., B. He, S. L. Chung, M. A. Menzies, and F. A. Frey (2004), Geologic, geochemical, and geophysical consequences of plume involvement in the Emeishan flood-basalt province, *Geology*, *32*(10), 917–920, doi:10.1130/G20602.1.

Xu, Y. G., B. He, X. L. Huang, Z. Y. Luo, D. Zhu, J. L. Ma, and H. Shao (2007), The debate over mantle plumes and how to test the plume hypothesis, *Earth Sci. Front.*, *14*(2), 1–9, doi:10.1016/S1872-5791(07)60011-6.

Xu, Y. G., Z. Y. Luo, X. L. Huang, B. He, L. Xiao, L. W. Xie, and Y. R. Shi (2008), Zircon U–Pb and Hf isotope constraints on crustal melting associated with the Emeishan mantle plume, *Geochim. Cosmochim. Acta*, *72*(13), 3084–3104, doi:10.1016/j.gca.2008.04.019.

Xu, Y. G., S. L. Chung, H. Shao, and B. He (2010), Silicic magmas from the Emeishan large igneous province, Southwest China: Petrogenesis and their link with the end-Guadalupian biological crisis, *Lithos*, *119*(1–2), 47–60, doi:10.1016/j.lithos.2010.04.013.

Zhang, Z. C., X. C. Zhi, L. Chen, A. D. Saunders, and M. K. Reichow (2008), Re–Os isotopic compositions of picrites from the Emeishan flood basalt province, China, *Earth Planet. Sci. Lett.*, *276*(1–2), 30–39, doi:10.1016/j.epsl.2008.09.005.

Zheng, L. D., Z. Y. Yang, Y. B. Tong, and W. Yuan (2010), Magnetostratigraphic constraints on two-stage eruptions of the Emeishan continental flood basalts, *Geochem. Geophys. Geosyst.*, *11*, doi:10.1029/2010gc003267.

Zhong, H., W. G. Zhu, Z. Y. Chu, D. F. He, and X. Y. Song (2007), Shrimp U–Pb zircon geochronology, geochemistry, and Nd–Sr isotopic study of contrasting granites in the Emeishan large igneous province, SW China, *Chem. Geol.*, *236*(1–2), 112–133, doi:10.1016/j.chemgeo.2006.09.004.

Zhong, H., I. H. Campbell, W. G. Zhu, C. M. Allen, R. Z. Hu, L. W. Xie, and D. F. He (2011), Timing and source constraints on the relationship between mafic and felsic intrusions in the Emeishan large igneous province, *Geochim. Cosmochim. Acta*, *75*(5), 1374–1395, doi:10.1016/j.gca.2010.12.016.

Zhou, M. F., J. Malpas, X. Y. Song, P. T. Robinson, M. Sun, K. Kennedy, C. Lesher, and R. R. Keays (2002), A temporal link between the Emeishan large igneous province (SW China) and the end-Guadalupian mass extinction, *Earth Planet. Sci. Lett.*, *196*(3–4), 113–122, doi:10.1016/S0012-821X(01)00608-2.

Zhou, M. F., P. T. Robinson, C. M. Lesher, R. R. Keays, C. J. Zhang, and J. Malpas (2005), Geochemistry, petrogenesis and metallogenesis of the Panzhihua gabbroic layered intrusion and associated Fe–Ti–V oxide deposits, Sichuan Province, SW China, *J. Petrol.*, *46*(11), 2253–2280, doi:10.1093/petrology/egi054.

Zhou, M. F., N. T. Arndt, J. Malpas, C. Y. Wang, and A. K. Kennedy (2008), Two magma series and associated ore deposit types in the Permian Emeishan large igneous province, SW China, *Lithos*, *103*(3–4), 352–368, doi:10.1016/j.lithos.2007.10.006.